

Preparation and characterization of protective self-cleaning TiO₂/kaolin composite coating

V. Jovanov^a✉, V. Zečević^b, T. Vulić^b, J. Ranogajec^b, E. Fidanchevska^a

a. Ss.Cyril and Methodius, University in Skopje, Faculty of Technology and Metallurgy, (Skopje, Republic of Macedonia)
b University of Novi Sad, Faculty of Technology, (Novi Sad, Serbia)

✉vojo@tmf.ukim.edu.mk

Received 20 August 2017
Accepted 16 January 2018
Available on line 18 July 2018

Abstract: The application of self-cleaning coatings presents one of the most effective ways to protect the surfaces of the building materials. The effect of TiO₂/kaolin based coatings applied to three types of substrates: non-porous, porous and highly porous, was investigated. Mechanical activation was applied for the impregnation of the active TiO₂ component (in content of 3 and 10 wt. %) into the kaolin support. Surface properties (roughness, hydrophilicity and micro-hardness) and functional properties (photocatalytic activity and self-cleaning efficiency) were studied in order to define the optimal formulation of the applied coatings. The effect of the photocatalytic behavior of the coated substrates in terms of self-cleaning ability was assessed by the photodegradation of Rhodamine B, performed before and after durability tests. The results obtained in this paper showed that photocatalytic activity of the TiO₂/kaolin composite coating generally depends on the procedure of TiO₂ impregnation into the kaolin clay and the loaded TiO₂ content.

KEYWORDS: Composite; Durability; Characterization; Microstructure; Particles size distribution; Scanning Electron Microscopy (SEM); X-ray diffraction (XRD)

Citation/Citar como: Jovanov, V.; Zečević, V.; Vulić, T.; Ranogajec, J.; Fidanchevska, E (2018) Preparation and characterization of protective self-cleaning TiO₂/kaolin composite coating. *Mater. Construcc.* 68 [331], e163 <https://doi.org/10.3989/mc.2018.08517>

RESUMEN: *Preparación y caracterización de un recubrimiento protector autolimpiante de TiO₂/caolín.* La aplicación de recubrimientos autolimpiantes presenta una de las maneras más efectivas de proteger las superficies de los materiales de construcción. Se ha investigado el efecto de recubrimientos basados en TiO₂/caolín, aplicados sobre tres tipos de sustratos: no poroso, poroso y altamente poroso. Se utilizó activación mecánica para la impregnación del componente de TiO₂ activo (en contenido del 3 y 10% en peso) sobre el soporte de caolín. Se han estudiado las propiedades superficiales (rugosidad, hidrofiliidad y microdureza) y las propiedades funcionales (actividad fotocatalítica y eficacia autolimpiante) para definir la formulación óptima de las capas aplicadas. El efecto del comportamiento fotocatalítico de los sustratos revestidos en términos de capacidad de autolimpieza se evaluó mediante la fotodegradación de Rodamina B, realizada antes y después de las pruebas de durabilidad. Los resultados obtenidos en este trabajo mostraron que la actividad fotocatalítica del revestimiento de TiO₂/caolín, dependen en general del procedimiento de impregnación de TiO₂ en la capa de caolín y el contenido utilizado de TiO₂.

PALABRAS CLAVE: Compuesto; Durabilidad; Caracterización; Microestructura; Distribución de tamaños de partículas de; Microscopía Electrónica de Barrido (MEB); Difracción de rayos X (DRX)

ORCID ID: V. Jovanov (<http://orcid.org/0000-0001-7734-0757>); V. Zecevic (<http://orcid.org/0000-0002-9825-4687>); T. Vulic (<http://orcid.org/0000-0001-9431-2846>); J. Ranogajec (<http://orcid.org/0000-0002-9831-2998>); E. Fidanchevska (<http://orcid.org/0000-0003-2919-5916>)

Copyright: © 2018 CSIC. This is an open-access article distributed under the terms of the Creative Commons Attribution 4.0 International (CC BY 4.0) License

1. INTRODUCTION

The surfaces of building materials (glass, ceramic and roofing tiles) used for outdoor applications are exposed to various kinds of environmental pollution which has intensified nowadays. In order to prevent the change of the structure of materials, to lengthen their service life and to keep a long-term esthetic appearance, coatings with self-cleaning properties have been applied (1,2). The utilization of nano TiO₂ (3,4) based coatings is among the widespread solutions used in the building sector, mainly because of their photocatalytic and hydrophilic properties. Over the past decades, many research studies have been carried out concerning the application of TiO₂ to different materials substrates used in construction but also for cultural heritage preservation (5-8). In addition to its proven photocatalytic properties, TiO₂ has chemical and biological inertness, high photochemical stability, and it is a low-price material (9). It is well known that agglomeration presents a considerable problem with the utilization of TiO₂ nano powder but its nanoparticles could also be spread in the environment (10). To overcome these problems, many studies regarding the immobilization of the TiO₂ on a suitable mineral support such as fly ash (11), zeolite (12), glass (13), quartz (14), cement (15), activated carbon nanofibers (16), polymeric matrix (17) and clays (18-22) have been carried out. The selected support should be compatible with the mineral substrates (such as cementitious materials, glass, ceramic tiles), but it should also be chemically inert. The participation of such support in chemical processes should facilitate pollutant elimination. Other requirements for a good photocatalyst support include large surface area and facile mass transport of the pollutants/degraded products to and from the active sites of the photocatalyst. The effective residence time of the photocatalyst also has to be increased and the blocking of the active sites has to be avoided (23).

Clay minerals (natural and synthetic) are promising support materials because of their high specific surface area, high absorption capacity, large pore volumes, chemical stability and good mechanical properties. TiO₂-clay nanocomposite enhances the decomposition of organic pollutants during photocatalytic degradation. In addition, it provides more active surface sites, reduces agglomerations and prevents nanoparticles from spreading in the environment. The immobilization of TiO₂ particles on the silicate layer of clay minerals can have a significant influence on the adsorption properties of the photocatalyst which is in direct correlation with the surface properties of the applied clay mineral (22). Layer double hydroxides (LDH) have been studied in the recent years as the catalyst support for TiO₂ because of their pronounced acid-base

and redox properties as well as their textural characteristics which can be tailored during synthesis (18,19). Natural clay minerals, like kaolinite (20), montmorillonite (21), halloysite (22) etc. present favorable supports for TiO₂ nanoparticles with the ability to promote the removal of organic compounds from waste water treatment. According to some authors (24,25) the nature of the substrate on which the coating is deposited presents an uncertain factor regarding the durability of a self-cleaning coating. This was the reason for the poor interest in self-cleaning coatings based on kaolin-TiO₂ considering their use in the field of building products. The aim of this study is to analyze and correlate different important characteristics of coatings such as: (i) the synthesis and characteristics of TiO₂-kaolin composites; (ii) the characteristics (surface and functional properties) of the coated mineral substrates (three different building materials with different values of water absorption coefficient(A): non-porous, $A = 1.04 \times 10^{-6} \text{ kg m}^{-2} \text{ min}^{-0.5}$; porous, $A = 0.73 \text{ kg m}^{-2} \text{ min}^{-0.5}$ and highly porous, $A = 8.22 \text{ kg m}^{-2} \text{ min}^{-0.5}$; and (iii) the durability characteristics (water rinsing and adhesion tape test) of the obtained self-cleaning coatings.

2. MATERIALS AND METHODS

2.1. Synthesis of the TiO₂/kaolin nanocomposite powders and suspensions

The TiO₂/kaolin composite powders were obtained by the impregnation of TiO₂ commercial suspension (in contents of 3 and 10wt.%) into a kaolin clay support. The commercial TiO₂ suspension used for this purpose (80 wt.% anatase and 20 wt.% rutile; grain size < 100 nm; content of dry matter $30.0 \pm 1.0 \text{ wt. \%}$ and pH 7) was obtained from Degussa company, Germany. The process of impregnation was carried out by mechanical activation in two different conditions of grinding. Firstly, the impregnation was performed in an attritor mill for 90 min at the speed of 1500 rpm. The second way of impregnation was carried out in a planetary mill during a period of 180 min at the speed of 200 rpm. The material/ball ratio was 1/5 in both procedures, while the pH value was in the range of 9 to 9.5. This pH value was maintained with the NaCO₃ and NaOH solutions, with concentrations of 0.67M and 2.25M, respectively. The obtained powders were dried at 105°C for 24 hours.

According to the TiO₂ content and the condition of impregnation, the obtained TiO₂/kaolin composite powders were labeled as E0A; E1A; E2A; E0P; E1P; E2P. The initial letter E indicates the kaolin clay used as support, numbers 0, 1 and 2 indicate the content of TiO₂ (0- without TiO₂, 1- 3.wt%TiO₂ and 2- 10wt.% TiO₂) while the last letter A / P indicate the attritor/ planetary mill conditions, respectively.

The obtained TiO₂/kaolin composite powders were used to make suspensions that later acted as protective coatings on mineral substrates. The composite suspension was formed by suspending 0.5g of TiO₂/kaolin composite powder into demineralized water (100 ml) using di-ammonia-hydrogen citrate as a dispersing agent. The suspension was stirred at 300 rpm, for 1hour. Ultrasonic bath (30 min) was used in order to prevent possible agglomeration.

Spray technique was applied for the deposition of the suspension onto the surface of the substrates under the following conditions: spraying pressure 6.5MPa, distance of the spray device from the sample 90cm, angle of spraying 45°, and diameter of nozzle 1.3mm. The coated substrates were afterwards dried at RT/24h.

2.2. Materials

Three types of mineral substrates were used as the medium for the application of the obtained suspensions as protective coatings. The first one, considered a porous system, was a clay roofing tile (CRT) produced in industrial conditions (Company NEXE Group) by extrusion, the second substrate was produced in laboratory conditions by pressing (P= 73MPa) using 60 wt.% of kaolin clay (35 wt% kaolinite) and 40 wt.% of fly ash obtained from the thermal power plant REK Bitola, Republic of Macedonia. The used fly ash influenced the increase of porosity of the mineral substrate (26) and it was considered as a high porous system in this investigation. The last substrate was a window glass (WG) used as a representative non-porous material. The substrates used in the investigation without coating are assigned as the reference using suffix R (CRT-R, CFA-R, WG-R), while the coated substrates were labelled by the suffix of the applied suspension (CRT-E2A, CRT-E2P, CAF-E2A, CAF-E2P, WG-E2A, WG-E2P).

2.3. Characterization methods

The particle size distribution of the TiO₂/kaolin composite powders was determined by Malvern Instruments, zeta-nanoseries, NanoZS under the following conditions: refraction index of the investigated suspensions (n=1.55), light absorption (a=0.3) and pH = 9. Additionally, a Malvern Mastersizer 2000 instrument was used for a more precise determination of the micro-size distribution of the particles from 0.02 to 2000 nm. For this measurement, the sample particles were dispersed in water with sodium pyrophosphate added with agitation and sonication until a stable dispersion was obtained.

The phase composition of the TiO₂/kaolin composite powders was determined by X-ray diffraction (Philips PW 1710). The investigations were done

under the following conditions: monochromatic CuK α radiation with $\lambda=1.5418 \text{ \AA}$ in the 5-55° of 2 θ range, scan rate 0.02°, 0.5 s per step.

The measurement of the contact angle values (Surface Energy Evaluation System, Advex Instruments, Brno, Czech Republic) was carried out with two experimental fluids: (distilled water and glycerol) before and after the water rinsing procedure and adhesion test. Droplets of the appropriate experimental fluid (cca 5 μl in volume) were gently deposited on the coated mineral substrate by micro syringe. The initial contact angle measurements (θ_{ci} , after 1s) were performed at five different points for each of the three specimens of the investigated mineral substrates. Each droplet deposited onto the surface of the mineral substrate was measured five times.

The surface roughness (Surtronic 25, Taylor Hobson) of the reference mineral substrates and of the coated samples, before and after water rinsing procedure and adhesion test, was evaluated based on the Ra parameter which represents the average roughness values obtained with a 4mm linear probe length. The obtained data were calculated according to ISO 4287 standard.

Before and after the water rinsing procedure and adhesion test, the Vickers micro-hardness values of the reference and of the coated samples were measured by Vickers micro-hardness technique (Microhardness tester model HVS 1000A, ZZV Precision Toll Supply) applying 0.3kg load.

The water absorption values by capillarity of the reference and the coated substrates were evaluated according to standard SRPS U. M8.300, 1985 – EN (27). The test samples (surface area of 60cm²) were dried until the constant mass (m_0) was reached, lateral sides of the samples were sealed with silicon, and placed in a vessel with demineralized water on the coated side. The samples were weighed (m_i) at determined time intervals (5min). The amount of water absorbed by the sample per unit area Q_i (kg/m²) at time t_i (s) was calculated as follows [1]:

$$Q_i = [(m_i - m_0) / S] \quad [1]$$

where:

S is the area of the sample in contact with water.

The capillary water absorption coefficient (A) was defined as the slope of the linear section of the curve obtained by plotting the mass change per area (Q_i) vs. the square root of time ($t_i^{1/2}$).

The photocatalytic activity of the synthesized powders (E0A; E1A; E2A; E0P; E1P; E2P) and that of the coated mineral substrates (before and after water rinsing and adhesion test) was investigated by monitoring the Rhodamine B (RhB) concentration change under the UV/VIS irradiation according to the procedures described in detail in (22).

The photocatalytic activity was estimated based on the efficiency of the RhB degradation. The photocatalytic activity A (%) was calculated according to the following relation [2]:

$$A (\%) = [(C_0 - C)/C_0] \cdot 100 \quad [2]$$

where:

C_0 presents the RhB solution concentration for the sample in the dark at defined time.

C presents the RhB solution concentration for the sample under UV/VIS light irradiation at defined time.

The RhB concentration was measured by UV-VIS spectrophotometer (EVOLUTION 600 spectrophotometer).

The assessment of the durability of the coated surfaces was carried out by using water rinsing test (as essential for self-cleaning of the coating) and tape adhesion test.

Water rinsing durability test was applied in order to examine the stability of three mineral substrates coated with the suspensions made of E2A / E2P nanocomposite powders in severe conditions (rain rinsing). Namely, the laboratory simulated rain rinsing procedure (19) was realized using the equipment which provides constant tap water flow (0.04 l/s) through a pipe system (nozzle diameter of 0.90mm) and water drop (height of 50 cm) on the sample (set at an angle of 45°). The duration of the test was 30 min.

A modified adhesion test according to the procedure for assessment of the porous models (15) was applied on the chosen substrates. A pressure sensitive tape (Scotch Tape, 3M) of defined dimensions was applied on the coated surface. The relative mass loss ($\Delta m/S$) after the application of the tape test was reported; where Δm presents the difference between

the mass of the tape measured after and before the test, while S presents the surface covered with the tape. The lower relative mass loss ($\Delta m/S$) indicates a better adhesion of the coating to the substrate surface.

The functional properties (photocatalytic activity and self-cleaning efficiency) of the coated samples were measured before and after the water rinsing and tape adhesion tests during UV/VIS irradiation. The Rhodamine B (10ppm) was used as the model pollutant for photocatalytic activity assessment, while the results of the contact angle measurements were used for the estimation of self-cleaning properties.

3. RESULTS AND DISCUSSION

3.1. Photocatalytic activity of the TiO₂/kaolin nanocomposite powders

The results of the photocatalytic activity of the obtained TiO₂/kaolin composite powders (E0A; E1A; E2A; E0P; E1P and E2P) obtained by monitoring the photocatalytic degradation of RhB during the period of 210min by UV/VIS irradiation are presented in Figure 1.

It is evident that composite powder E2A has the highest photocatalytic activity value (65%), while the composite powder E2P has the lowest one (55%).

Regarding the TiO₂ content impregnated into the kaolin clay support, the samples impregnated with 10% TiO₂ showed significantly higher photocatalytic activity than the samples impregnated with 3% TiO₂, while the samples treated under the same conditions without impregnated TiO₂ showed no photocatalytic activity under the UV/VIS irradiation (28).

Depending on the type of mill, during the process of impregnation, the TiO₂/kaolin composite

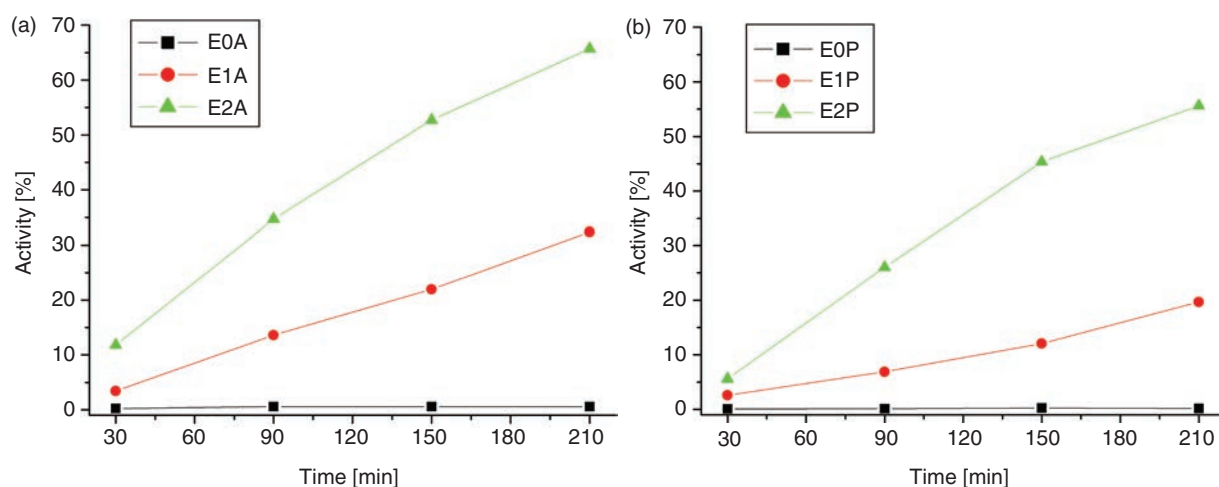


FIGURE 1. Photocatalytic activity values of the TiO₂/kaolin composite powders: (a) E0A; E1A and E2A (attritor mill) and (b) E0P; E1P and E2P (planetary mill).

powders obtained in an attritor mill showed higher photocatalytic activity (for 10%) than those impregnated in a planetary mill. Based on those preliminary photocatalytic activity results, the TiO₂/kaolin composite powders E2A and E2P were additionally characterized and used for the creation of photocatalytic suspensions which were further applied on the chosen mineral supports (28).

3.2. Particle size distribution of the TiO₂/kaolin composite powders

Particle size distribution of the most photocatalytic active TiO₂/kaolin composite powders i.e. E2A and E2P is presented in Figure 2.

It is evident that E2A powder (10wt.% TiO₂/ attritor mill) possesses a three modal particle size distribution with the following maximal particle diameters: 50nm, 255nm and 1700nm, while the E2P powder (10wt.% TiO₂/ planetary mill) has bimodal particle size distribution with maximal particle diameters of 217 nm and 1138nm. The small fraction of the particles with the average diameter

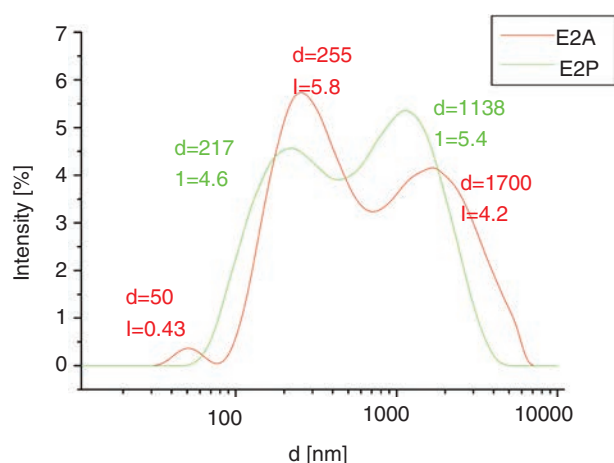


FIGURE 2. Particle size distribution of the E2A and E2P powders, determined by a Malvern Instruments zeta-nanosizer.

size smaller than 100 nm were obtained only in the case of the impregnation in an attritor mill, which is evidently the reason for the better photocatalytic behavior of this powder in comparison with the powder obtained by the impregnation in a planetary mill. Also, it was noticed that both powders had particles distributed in micro-size range, Figure 3. The micro-sized distribution of the powders could present some difficulties regarding their stability, but since the attempt of this work was to develop a coating with appropriate compatibility to the used mineral substrate, the micro-size of the powder particles did not present a great disadvantage.

3.3. Phase composition of TiO₂/kaolin composite powders

The phase composition of both E2A and E2P powders are shown in Figure 4. Mainly, kaolinite phase appears as the dominant phase followed by quartz and Na₂CO₃ used in the milling procedure. The presence of anatase is evident in both samples, while the rutile phase of TiO₂ was not identified. Based on the obtained diffraction patterns, it can be concluded that the different way of TiO₂ impregnation did not modify the initial structure of the clay mineral and of the TiO₂ phase.

3.4. Characterization of the coated mineral substrates

The values of average capillary water absorption coefficient presented in Table 1 were used in order to estimate the water absorption value of the different mineral substrates by capillary phenomenon for both the reference samples and coated samples. As expected, the CFA-R (sample based on clay material and fly ash) substrate showed the highest value of capillary water absorption coefficient, due to the highest porosity due to the presence of fly ash (26,18). The glass (WG) substrates as non-porous materials, showed a negligible capillary water absorption.

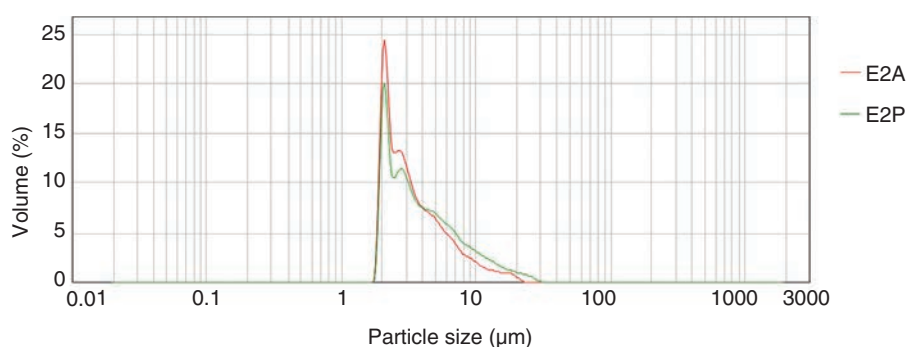


FIGURE 3. Particle size distribution of the E2A and E2P powders, determined by a Malvern Mastersizer 2000 instrument.

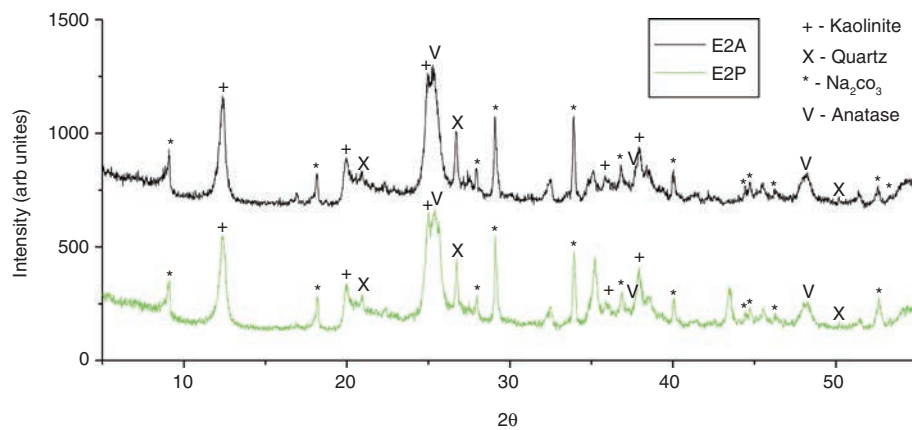


FIGURE 4. XRD patterns of composite powders E2A and E2P.

TABLE 1. Average capillary water absorption coefficient (A) for the reference mineral substrates and for the coated substrates

| Mineral substrate | A [kg/m ² min ^{1/2}] |
|-----------------------------|--|
| Clay roofing tile, CRT | |
| CRT-R | 0.73 |
| CRT-E2A | 0.59 |
| CRT-E2P | 0.63 |
| Clay-fly ash composite, CFA | |
| CFA-R | 8.22 |
| CFA-E2A | 6.43 |
| CFA-E2P | 6.45 |
| Window glass, WG | |
| WG-R | 1.04x10 ⁻⁶ |
| WG-E2A | 1.03x10 ⁻⁶ |
| WG-E2P | 1.03x10 ⁻⁶ |

After the deposition of the coating on to the mineral substrates, the average capillary water absorption coefficient decreased for all the examined substrate samples (19). This decrease was low for the CRT sample, but more pronounced for the CFA substrate. No significant difference between the samples coated with different suspensions was noticed. The WG substrate samples after the coating procedure still possessed a negligible capillary water absorption coefficient.

The comparison of the surface properties (surface roughness and Vickers micro-hardness), before and after the application of both coatings (E2A / E2P), provided the opportunity to investigate the surface changes which evidently had a great influence on the functional properties of the coated samples.

Surface roughness values (Ra parameter) were used for evaluating the surface roughness of the reference and coated substrates. The values

obtained for Ra are presented in Table 2. After the deposition of the coatings, a slight increase of the surface roughness value was noticed for the WG substrates. Evidently, the initial higher roughness of the CFA-R and CRT-R substrates made an appropriate deposition of the coatings difficult and consequently, the obtained difference of the Ra values between the reference and the coated samples was negligible (18).

The results of the Vickers micro-hardness (HV) test presented in Table 3, indicate an insignificant improvement of the micro-hardness after the application of both coatings to the substrates. This could be mainly attributed to the higher amount of crystalline particles on the coated substrates (19).

The results of the average initial contact values q_{ci} of the reference substrates (CRT-R, CFA-R and WG-R) and of the coated substrates (CRT-E2A, CRT-E2P, CFA-E2A, CFA-E2P, WG-E2A and WG-E2P) are presented in Table 4. The values of the q_{ci} of the reference substrates are lower than 90°, which confirms that all the substrates are hydrophilic. After the deposition of the coatings (E2A/E2P) on the substrates, the contact angle generally decreased increasing the surface hydrophilicity of the substrates (18,19). The value of the q_{ci} decreased for almost 60% when the WG substrates were coated. It is worth noticing that the contact angle measurements for CRT and WG substrate samples were performed with water as a working liquid, while for the CFA samples they were performed with glycerol. Due to the high values of capillary absorption of the CFA substrate, the applied drops of water instantly penetrated into the substrate so that it was impossible to measure the contact angle values by using water as a working fluid. The coating obtained by the impregnation in a attritor mill showed higher hydrophilicity (lower contact angle) for all the studied substrates than the coating obtained by the impregnation in a planetary mill.

TABLE 2. Surface roughness values (Ra parameter)

| Mineral substrate | Ra [μm] | | |
|-----------------------------|---------------------------------|--|--|
| | Reference and coated substrates | Coated substrates after tape adhesion test | Coated substrates after water rinsing test |
| Clay roofing tile, CRT | | | |
| CRT-R | 2.45 | - | - |
| CRT-E2A | 2.50 | 2.47 | 2.45 |
| CRT-E2P | 2.55 | 2.50 | 2.45 |
| Clay-fly ash composite, CFA | | | |
| CFA-R | 12.31 | - | - |
| CFA-E2A | 12.24 | 12.25 | 12.27 |
| CFA-E2P | 12.26 | 12.28 | 12.30 |
| Window glass, WG | | | |
| WG-R | 0.09 | - | - |
| WG-E2A | 0.21 | 0.18 | 0.09 |
| WG-E2P | 0.27 | 0.24 | 0.09 |

TABLE 3. Vickers micro-hardness (HV) values

| Mineral substrate | Vickers micro-hardness, HV | | |
|-----------------------------|---------------------------------|--|--|
| | Reference and coated substrates | Coated substrates after tape adhesion test | Coated substrates after water rinsing test |
| Clay roofing tile, CRT | | | |
| CRT-R | 45.0 | - | - |
| CRT-E2A | 45.8 | 45.5 | 45.5 |
| CRT-E2P | 45.5 | 45.3 | 45.3 |
| Clay-fly ash composite, CFA | | | |
| CFA-R | 13.3 | - | - |
| CFA-E2A | 13.7 | 13.5 | 13.7 |
| CFA-E2P | 13.4 | 13.4 | 13.4 |
| Window glass, WG | | | |
| WG-R | 453.0 | - | - |
| WG-E2A | 456.3 | 453.8 | 453.0 |
| WG-E2P | 455.7 | 453.5 | 453.0 |

3.5. Self-cleaning and photocatalytic properties of the coated mineral substrates

The self-cleaning properties of the coated substrates assessed by the measurement of the initial contact angle q_{ci} are presented in Figure 5. The evident decrease of the initial contact angle values during UV/VIS irradiation is consistent with other similar studies (18). This fact proved the existence of the self-cleaning effect of the applied coatings (E2A and E2P) on both types of substrates, porous and non-porous.

The results of the evaluation of photocatalytic activity based on the RhB degradation efficiency, with UV/VIS irradiation, are presented in Fig. 6. The obtained results showed a significant photocatalytic

activity for the coatings E2A/ E2P applied to the CRT and WG substrates, but a negligible activity for the CFA substrate (only 3.5% for E2P and 5% for E2A after 24h of UV/VIS irradiation). The present phenomenon was directly correlated to the surface properties and porosity of the substrates (Tables 1, 2 and 3). Namely, the high porosity and high capillary water absorption of the CFA substrate enables the entering of the active suspension deep into the material, disabling the activation by light inside the material, leaving only the small remaining amount of the suspension deposited on the surface of the material capable of photocatalytic reacting. The evident low photocatalytic activity of the coatings applied on the CFA substrate made this substrate unsuitable for further investigations regarding the

durability tests. The glass substrates (WG) as non-porous samples showed almost the same photocatalytic activity for both coatings (E2A/E2P) during the period of 24 hours. In the case of the CRT substrates, the difference between two types of coatings is evident. Namely, up to 3.5h of UV/VIS irradiation, both coatings applied to this substrate had the same activity. However, after 24h of UV/VIS irradiation, the activity was 42% higher in the case of the coating composed of E2A powder. As standard UNI 11259:2008 (29) and literature reference (30) state (where Rhodamine B is used as a model pollutant), a photocatalytic material can be considered active if its efficiency reaches 20% after 4 hours and 50% after 26h of UV irradiation. According to this, it can be concluded that both coatings (E2A and E2P) on the WG substrate can be considered

as photocatalytic materials because after 4h they showed the activity of 48% and 47%, respectively. In addition, after just 24 h they showed the activity of 90 % and 88 %, respectively. The E2A coating deposited on the CRT substrate showed the activity of 13% after 4 hours, but after 24 h the test was stopped. However, after only 24h its efficiency was 43% with the tendency to rise thus proving its good catalytic property.

3.6. Durability testing of photocatalytic coatings

The results of the modified tape adhesion test presented in Table 5 indicate good adhesion durability due to a low mass loss of the coated substrates in the case of the CRT and CFA substrates. For the WG samples a more significant mass loss was detected than in the case of the two samples specified above.

The comparisons of the surface roughness values, Ra parameter, for the three types of samples before and after the application of the tape adhesion test and water rinsing durability test are presented in Table 2. No significant changes were found, except in the case of the WG coated samples after the rinsing test, where the coating was almost completely removed. Additionally, a negligible decrease of the micro-hardness value after the applied durability tests for both types of suspensions was identified, Table 3.

The results of the θ_{ci} of the coated CRT, as the function of UV/VIS irradiation time before and after durability (water rinsing and tape adhesion) tests are presented in Figure 7

(a and b). It is evident that there was a significant increase of θ_{ci} for both E2A and E2P coatings, applied on CRT substrate, after the durability test.

TABLE 4. Average initial contact angle values q_{ci}

| Mineral substrate | Average initial contact angle θ_{ci} (°) |
|-----------------------------|---|
| Clay roofing tile, CRT | Water as a working liquid |
| CRT-R | 54.7 |
| CRT-E2A | 36.99 |
| CRT-E2P | 38.97 |
| Clay-fly ash composite, CFA | Water as a working liquid |
| CFA-R | 52.56 |
| CFA-E2A | 35.29 |
| CFA-E2P | 37.92 |
| Window glass, WG | Glycerol as a working liquid |
| WG-R | 67.02 |
| WG-E2A | 27.40 |
| WG-E2P | 28.73 |

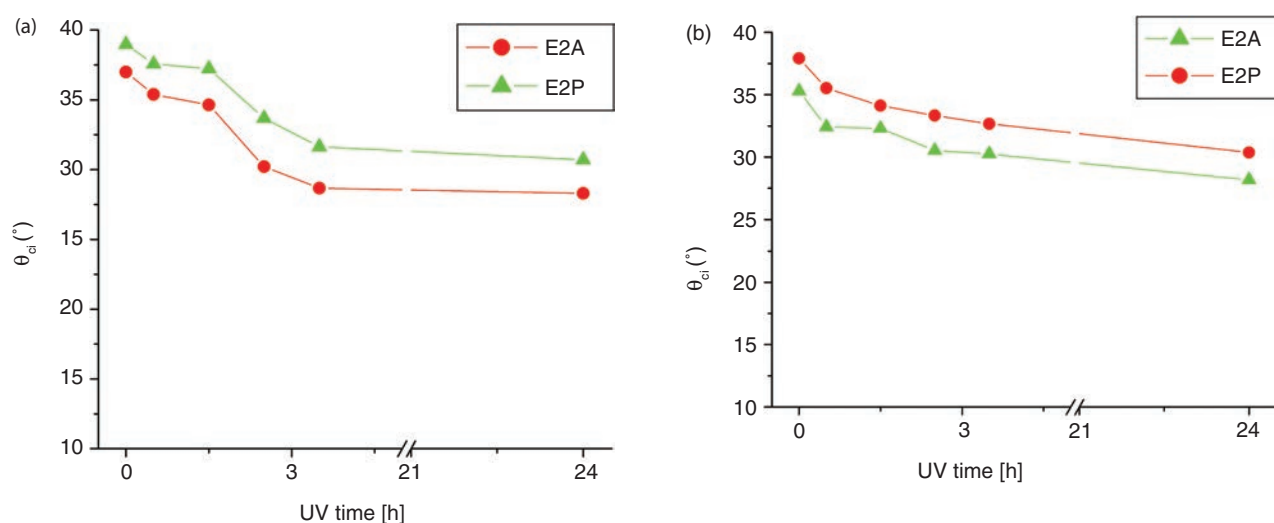


FIGURE 5. Initial contact angle of E2A and E2P coatings applied to: (a) CRT substrate, (b) CFA substrate and (c) WG substrate as the function of UV/VIS irradiation time.

TABLE 5. The relative mass loss ($\Delta m/S$) after the application of modified tape test

| Mineral substrate | Sample | $\mu m/S$ [$\mu g/cm^2$] |
|-------------------|---------|----------------------------|
| CRT | CRT-R* | 77.7 |
| | CRT-E2A | 64.5 |
| | CRT-E2P | 65.7 |
| CFA | CFA-R* | 262 |
| | CFA-E2A | 248 |
| | CFA-E2P | 255 |
| WG | WG-R* | 18.2 |
| | WG-E2A | 26.8 |
| | WG-E2P | 30.4 |

* The tape takes off only the deposited powder (dust) from the atmosphere

The increase of θ_{ci} was more pronounced after the water rinsing procedure for both coatings had been applied to the CRT substrate, having its maximum at the start of the experiment (without UV/Vis irradiation).

As a result of very low resistance towards rinsing with water of both E2A and E2P coatings applied on WG substrate, (Table 2), the θ_{ci} and photocatalytic degradation efficiency values were measured only after tape adhesion durability test, Figure 7 (c and d). Obviously, there was a slight increase of θ_{ci} value after the tape adhesion test (without the influence of UV/Vis irradiation), but during UV/Vis irradiation a significant decrease of θ_{ci} value was evident.

The increase of the θ_{ci} value of both CRT and WG coated substrates after the applied durability

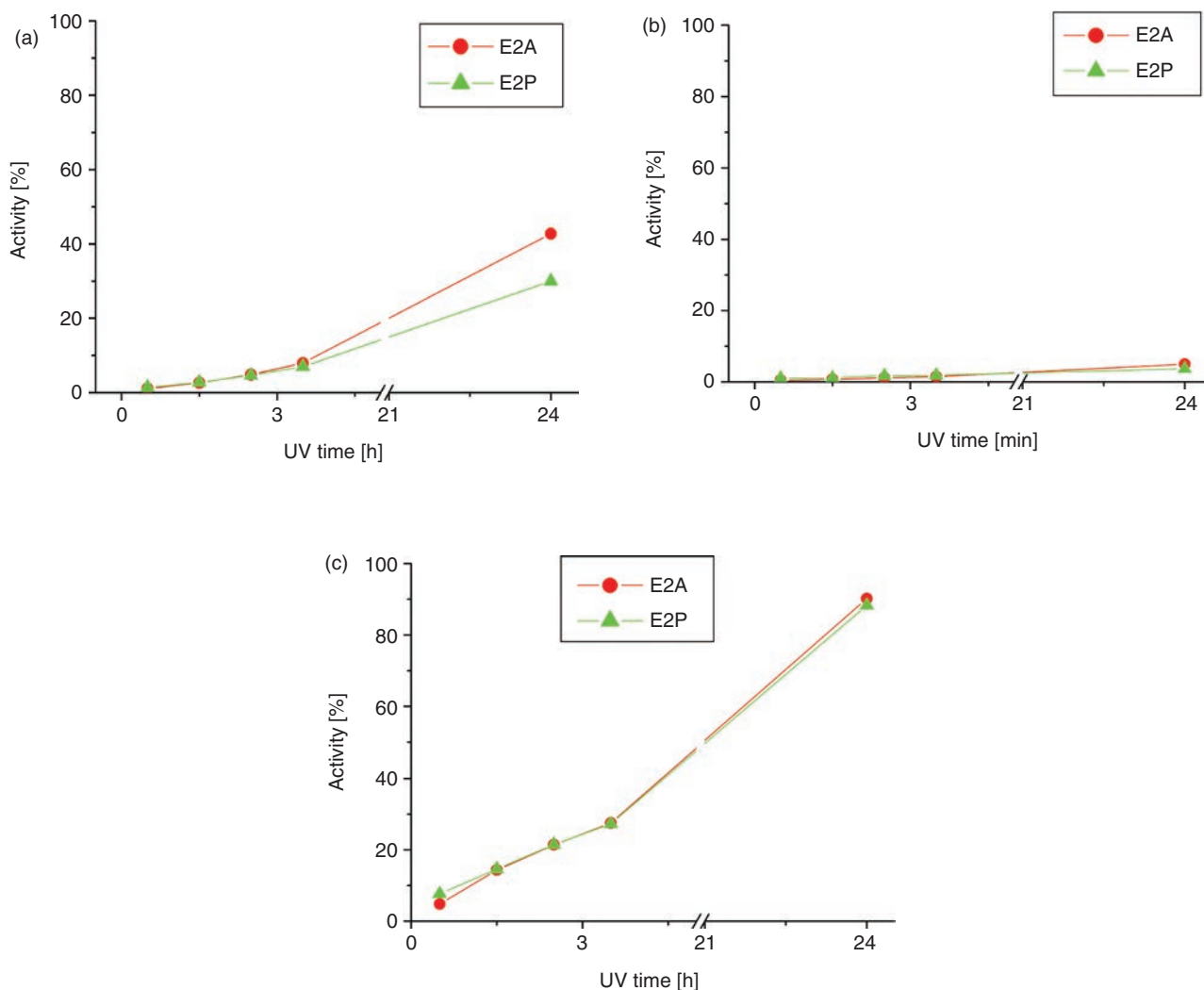


FIGURE 6. Photocatalytic activity of the coating composed of E2A and E2P composite powder and applied to: (a) clay roofing tile (CRT), (b) composite material (CFA) and (c) window glass (WG).

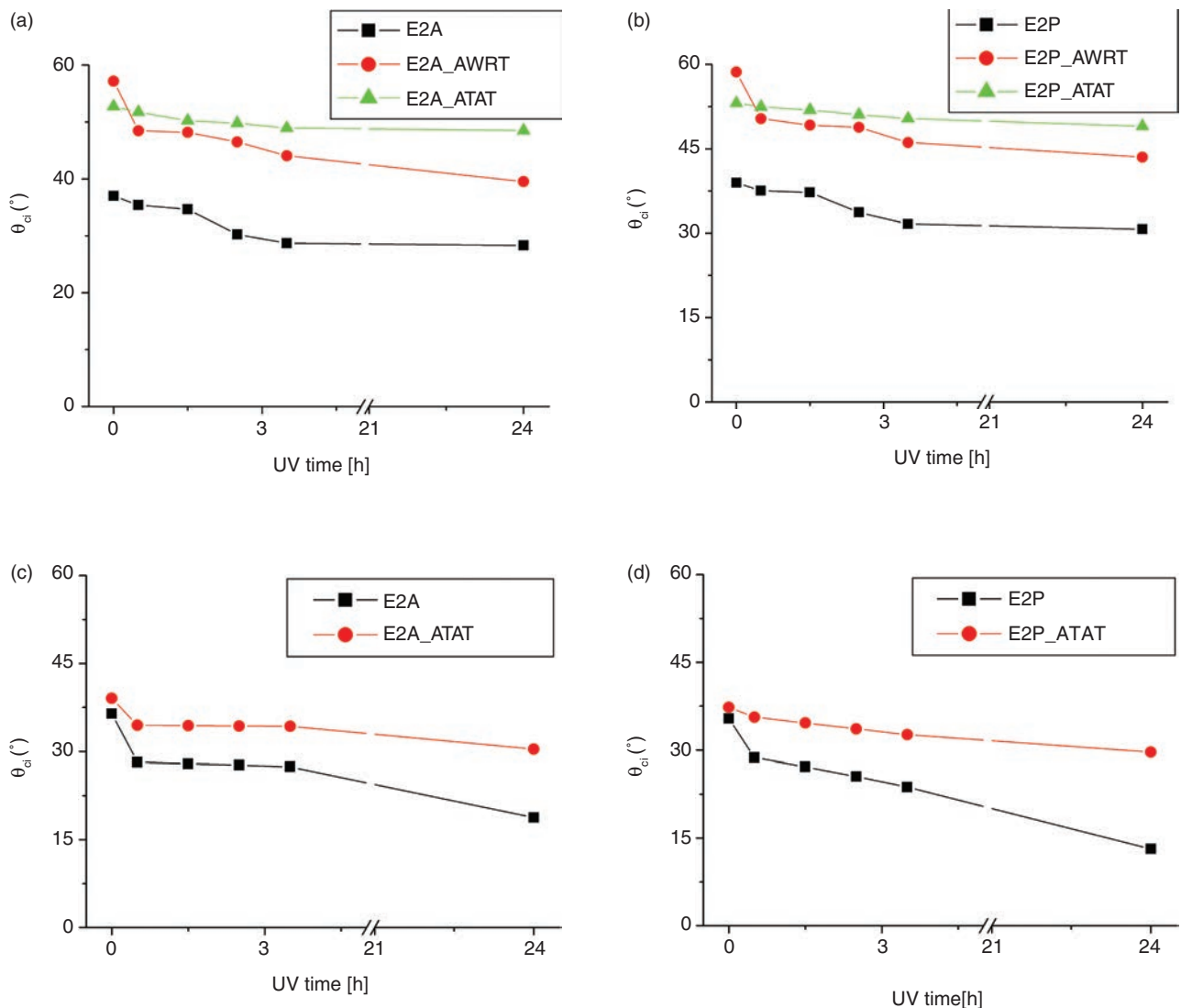


FIGURE 7. Self-cleaning efficiency assessment: a. CRT-E2A, b. CRT-E2P, c. WG-E2A, d. WG-E2P, (E2A and E2P – substrates with coating; AWRT- after water rinsing test; ATAT- after tape adhesion tests).

tests (without the influence of UV/VIS irradiation) could be the result of the physical removal of the deposited coatings and of the changes of the surface morphology during the performing durability tests. The existence of a decreasing trend line of the θ_{ci} value as the function of UV/VIS irradiation after the durability tests of the analyzed coatings suggests that a considerable self-cleaning efficiency still exists.

The results of photocatalytic degradation efficiency of Rhodamine B with UV/VIS irradiation before and after the appropriate durability tests of the coated CRT and WG substrates are presented in Figure 8. It is evident that up to 2.5h of UV/Vis irradiation, the photocatalytic activity was almost the same before and after the durability

tests (water rinsing and tape adhesion tests) for the coated CRT substrates. Nevertheless, by increasing the time of UV/Vis irradiation up to 24h, the photocatalytic activity decreased down to 29% for the CRT-E2A sample after both durability tests. Even more prominent decrease was evident for the CRT-E2P sample, i.e. up to 17,5% after tape adhesion test and 15,5% after water rinsing test. In the case of the WG-E2A and WG-E2P samples, a more significant decrease of photocatalytic activity values was noticed after 24h of UV/Vis irradiation: up to 54% and 47% respectively, after tape adhesion test, Figure 8 (c and d).

According to the presented results, it can be concluded that both coatings exhibited relatively good durability when they were applied to CRT

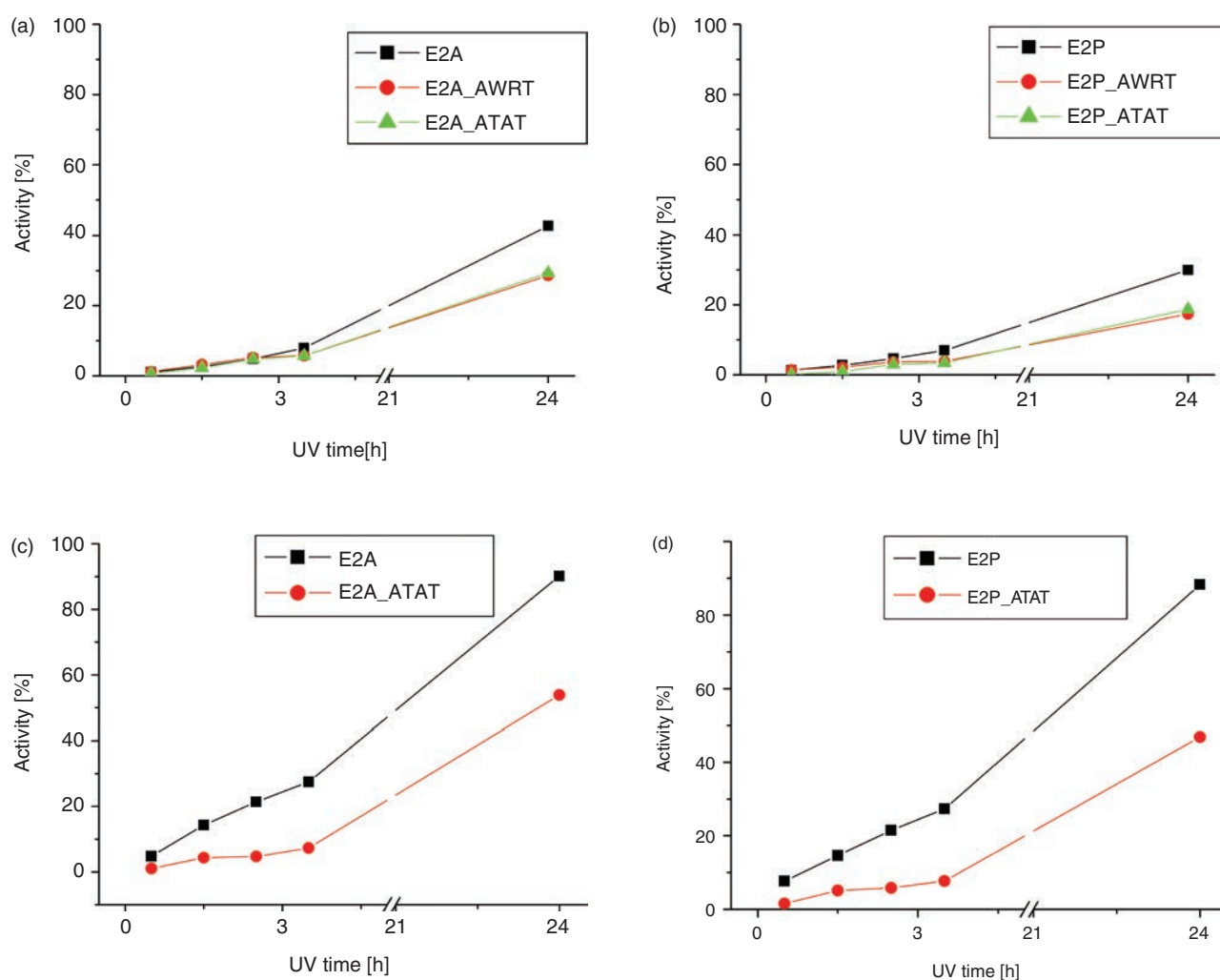


FIGURE 8. Photocatalytic activity assessment: a. CRT-E2A, b. CRT-E2P, c. WG-E2A, d. WG-E2P (E2A and E2P – substrates with coating; AWRT- after water rinsing test, ATAT- after tape adhesion tests).

and WG substrates. The coating composed of E2A powder and applied on WG substrate showed better photoactivity after durability tests, suggesting good compatibility and stability with this substrate, which is in good correlation with other reported studies (29,30).

CONCLUSIONS

The research showed that photocatalytic activity results of the obtained TiO₂/supported kaolin powders greatly depend on the TiO₂ impregnation into the kaolin clay procedure and on the content of the TiO₂ loading.

Based on comparative investigation, it was evident that the samples impregnated by mechanical activation in an attritor and planetary mill possessed mainly micro-sized particle distribution. The impregnation of the TiO₂ by mechanical activation

in an attritor mill leads to the formation of small fractions of nano-sized particles with an average diameter of 50 nm, which resulted in a more pronounced photocatalytic activity of these composites.

Similar trend was also noticed for the deposited coatings. The coating obtained from the powder impregnated with the highest amount of TiO₂ in an attritor mill also had the highest hydrophilicity (lower contact angle) and was potentially more efficient in the removal of the pollutant from the studied substrates (window glass and industrial clay roofing tile) than the coating prepared with the powder containing the same amount of TiO₂, but impregnated in a planetary mill. This fact is in correlation with the values of particle size distribution and their stability.

The procedure for the preparation of the TiO₂/kaolin composite photocatalyst presented in this study, the achieved durability and the

negligible influence of the deposited photocatalytic TiO₂/kaolin composite coating on surface properties (surface roughness, Vickers micro-hardness and contact angle values) present an advantageous and very important argument for further investigation in this field.

ACKNOWLEDGEMENT

The financial support from Serbian Ministry of Education, Science and Technological Development (Contract No. III45008) is gratefully acknowledged.

REFERENCES

- Chen, J.; Poon, C.S. (2009) Photocatalytic construction and building materials: from fundamentals to applications. *Build. Environ.* 44 (9), 1899–1906. <https://doi.org/10.1016/j.buildenv.2009.01.002>
- Ducman, V.; Petrović, V.; Škapin, D.S. (2013) Photocatalytic efficiency of laboratory made and commercially available ceramic building products. *Ceram. Int.* 39 (3), 2981–2987. <https://doi.org/10.1016/j.ceramint.2012.09.075>
- Goffredo, G.B.; Munafò, P. (2015) Preservation of historical stone surfaces by TiO₂ nanocoatings. *Coatings*. 5 (2), 222–231. <https://doi.org/10.3390/coatings5020222>
- Sciancalepore, C. F.; Bondioli, F. (2015) Durability of SiO₂-TiO₂ photocatalytic coatings on Ceramic Tiles. *Int. J. Appl. Ceram. Technol.* 12 (3), 679–684. <https://doi.org/10.1111/ijac.12240>
- Sciancalepore, C.; Manfredini, T.; Bondioli, F. (2014) Antibacterial and self-cleaning coatings for silicate ceramics: A review. *Advances in Science and Technology*, 92, 90–99. <https://doi.org/10.4028/www.scientific.net/AST.92.90>
- Pal, S.; Contaldi, V.; Liccillulli, A.; Marzo, F. (2016) Self-cleaning mineral paint for application in architectural heritage. *Coatings*. 6 (4), 48. <https://doi.org/10.3390/coatings6040048>
- Taurino, R.; Barbieri, L.; Bondioli, F. (2016) Surface properties of new green building material after TiO₂-SiO₂ coatings deposition. *Ceram. Int.* 42 (4), 4866–4874. <https://doi.org/10.1016/j.ceramint.2015.12.002>
- Ranogajec, J.; Radeka, M.; Bačkalić, Z.; Škapin, A.; Zorić, D. (2010) Photocatalytic and superhydrophilic phenomena of TiO₂ coated clay roofing tiles. *Chem. Ind. Chem. Eng. Q.* 16 (2), 117–126. <https://doi.org/10.2298/CICEQ091214018R>
- Zhang, Y.H.; Gan, H.; Zhang, G. (2011) A novel mixed-phase TiO₂/kaolinite composites and their photocatalytic activity for degradation of organic contaminants. *Chem. Eng. J.* 172 (2–3), 936–943. <https://doi.org/10.1016/j.cej.2011.07.005>
- Warheit, D.B.; Hoke, R.A.; Finlay, C.; Donner, E.M.; Reed, K.L.; Sayes, C.M. (2007) Development of a base set of toxicity tests using ultrafine TiO₂ particles as a component of nanoparticle risk management. *Toxicol Lett.* 2007. 171(3), 99–110. <https://doi.org/10.1016/j.toxlet.2007.04.008>
- Yu, Y. (2004) Preparation of nanocrystalline TiO₂-coated coal fly ash and effect of iron oxides in coal fly ash on photocatalytic activity. *Powder Technol.* 146 (1–2), 154–159. <https://doi.org/10.1016/j.powtec.2004.06.006>
- Yahiro, H.; Miyamoto, T.; Watanabe, N.; Yamaura, H. (2007) Photocatalytic partial oxidation of *a*-methylstyrene over TiO₂ supported on zeolites. *Catal. Today*, 120 (2), 158–162. <https://doi.org/10.1016/j.cattod.2006.07.039>
- Puzenat, E.; Puerre, P. (2003) Studying TiO₂ coating on silica-covered glass by O₂ photosorption measurements and FTIR-ATR spectrometry: Correlation with the self-cleaning efficacy. *J. Photochem. Photobiol. A: Chemistry*, 160 (1–2), 127–133
- Rebilasová, S.; Mamulová, K.K.; Matějka, V.; Tokarský, J.; Kukutschová, J.; Neuwirthová, L.; ČAPKOVÁ, P. (2010) Preparation, characterization and comparison of composites: kaolinite/TiO₂ and quartz/TiO₂. *NANOCON'10 International conference*, Czech Republic
- Vulic, T.; Hadnadjev-Kostic, M.; Rudic, O.; Radeka, M.; Marinkovic-Neducin, R.; Ranogajec, J. (2013) Improvement of cement-based mortars by application of photocatalytic active Ti–Zn–Al nanocomposites. *Cem. Concr. Compos.* 36, 121–127. <https://doi.org/10.1016/j.cemconcomp.2012.07.005>
- Keller, N.; Rebmann, G.; Barraud, E.; Zahraa, O.; Keller, V. (2005) Macroscopic carbon nanofibers for use as photocatalytic support. *Catal. Today* 101, 323–329. <https://doi.org/10.1016/j.cattod.2005.03.021>
- Portela, R.; Sánchez, B.; Coronado, J.M.; Candal, R.; Suárez, S. (2007) Selection of TiO₂-support: UV-transparent alternatives and long-term use limitations for H₂S removal. *Catal. Today* 129 (1–20), 223–230. <https://doi.org/10.1016/j.cattod.2007.08.005>
- Rudic, O.; Rajnovic, D.; Cjepa, D.; Vucetic, S.; Ranogajec, J. (2015) Investigation of the durability of porous mineral substrates with newly designed TiO₂-LDH coating. *Ceram. Int.* 41 (8), 9779–9792. <https://doi.org/10.1016/j.ceramint.2015.04.050>
- Rudic, O.; Ranogajec, J.; Vulic, T.; Vucetic, S.; Cjepa, D.; Lazar, D. (2014) Photo-induced properties of TiO₂/ZnAl layered double hydroxide coating onto porous mineral substrates. *Ceram. Int.* 40 (7), Part A 9445–9455. <https://doi.org/10.1016/j.ceramint.2014.02.017>
- Chong, M.N.; Vimonses, V.; Lei, S.; Jin, B.; Chow, C.; Saint, C. (2009) Synthesis and characterisation of novel titania impregnated kaolinite nano-photocatalyst. *Microporous Mesoporous Mater.* 117 (1–2), 233–242. <https://doi.org/10.1016/j.micromeso.2008.06.039>
- Yuan, L.; Huang, D.; Guo, D.; Yang, Q.; Yu, J. (2011) TiO₂/montmorillonite nanocomposite for removal of organic pollutant. *Appl. Clay Sci.* 53 (2), 272–278. <https://doi.org/10.1016/j.clay.2011.03.013>
- Szczepanik, B. (2017) Photocatalytic degradation of organic contaminants over clay-TiO₂ nanocomposites: A review. *Appl. Clay Sci.* 141, 227–239. <https://doi.org/10.1016/j.clay.2017.02.029>
- Fujishima, A.; Hashimoto, K.; Watanabe, T. (1999) *TiO₂ photocatalysis fundamentals and applications*, Tokyo Bk (1999).
- Ma, Y.; Qiu, J.B.; Cao, Y.A.; Guan, Z.S.; Yao, J.N. (2001) Photocatalytic activity of TiO₂ films grown on different substrates. *Chemosphere - Oxford* 44 (5), 1087–1092.
- Yu, J.; Zhao, X. (2000) Effect of substrates on the photocatalytic activity of nanometer TiO₂ thin films. *Mater. Res. Bull.* 35 (8), 1293–1301. [https://doi.org/10.1016/S0025-5408\(00\)00327-5](https://doi.org/10.1016/S0025-5408(00)00327-5)
- Fidanchevska, E.; Jovanov, V.; Angjushva, B.; Srebrenkoska, V. (2014) Composites based on fly ash and clay, The 27-th Conference of the Israel Nuclear Societies, February, 11–13, Dead Sea Israel
- SRPS U.M.8.300:1985, Determination of the Capillary Water Absorption of Building Material and Coatings, 1985.
- Jovanov, V.; Rudic, O.; Ranogajec, J.; Fidanchevska, E. (2017) Synthesis of nanocomposite coating based on TiO₂/ZnAl layer double hydroxides. *Materiales de Construcción* 67(325), 112–120. <https://doi.org/10.3989/mc.2017.07215>
- UNI 11259:2008. Determination of the photocatalytic activity of hydraulic binders – Dodamina test method. Ente nazionale italiano di unificazione; 2008
- Cassar, L.; Beeldens, A.; Pimpinelli, N.; Guerrini, G.L. (2007) Photocatalysis of cementitious materials. *Proceedings pro055: International RILEM symposium on photocatalysis, environment and construction materials – TDP 2007*, Edited by: Bigliani, P., Cassa, L., RILEM Publications SARI. 131–45